Partially Bridge-Fluorinated Dimethyl Bicyclo[1.1.1]pentane-1,3-dicarboxylates: Preparation and NMR Spectra

Alexander B. Shtarev,[†] Evgueni Pinkhassik,[†] Michael D. Levin,[†] Ivan Stibor,[‡] and Josef Michl*,[†]

Contribution from the Department of Chemistry and Biochemistry, University of Colorado, Boulder, Colorado 80309-0215, and Department of Organic Chemistry, Institute of Chemical Technology, Technická 5, 16628 Prague, Czech Republic

Received January 3, 2000

Abstract: Direct fluorination of dimethyl bicyclo[1.1.1]pentane-1,3-dicarboxylate, obtained from [1.1.1]propellane prepared by an improved synthetic procedure, furnished esters of 14 of the 15 possible bridge-fluorinated bicyclo[1.1.1]pentane-1,3-dicarboxylic acids, isolated by preparative GC. Calculated geometries reflect the substitution pattern in a regular fashion compatible with Bent's rules. Considerable additional strain is introduced into the bicyclo[1.1.1]pentane cage by polyfluorination; it is calculated to be as high as 33−35 kcal/mol for hexasubstitution. Three arrangements of the fluorine substituents are especially strain-rich: geminal, proximate, and W-related. The ^{1}H, ^{13}C, and ^{19}F NMR spectra exhibit a striking variety of chemical shifts and long-range coupling constants. These are in good agreement with results calculated with neglect of the bridgehead substituents for all of the chemical shifts by the GIAO-RHF/6-31G*//RHF/6-31G* and GIAO-RHF/6-31G*//MP2/6-31G* methods and for many of the coupling constants by the EOM-CCSD/6-311G*//MP2/6-311G* method. The proximate $^{4}J_{FF}$ constants are particularly large (50−100 Hz) and show an inverse linear dependence on the calculated F−F distance in the range 2.43−2.58 Å.

Introduction

We report the direct fluorination of dimethyl bicyclo[1.1.1]-pentane-1,3-dicarboxylate (**0**) to prepare its monofluoro (**1**), all four difluoro (**2a**, **2x**, **2y**, **2z**), all four trifluoro (**3a**, **3x**, **3y**, **3z**), and three of the four possible tetrafluoro (**4a**, **4x**, **4z**) derivatives carrying fluorine on the methylene bridges (Figure 1). The tetrafluorinated isomer **4y** was not formed in detectable amounts. The pentafluorinated (**5**) and hexafluorinated (**6**) diesters have already been reported.[1]

Fluorinated bicyclo[1.1.1]pentanes are of interest to us since (i) bridge fluorination may provide a simple means of modifying the remarkable properties of the highly strained yet very stable bicyclo[1.1.1]pentane cage,[2] such as the long-distance propagation of bridgehead spin density,[3] and (ii) the unusual variety of long-range NMR coupling constants in **5** and **6** suggested[1] that the compounds **1**−**6** will offer both an ideal testing ground for the ability of current ab initio methods to compute these quantities and an opportunity to uncover their empirical relations to molecular structure. Besides, little is known about the relative rates of hydrogen substitution in direct fluorination of small-ring hydrocarbons,[4] and the structure elucidation of the up to 13 anticipated previously unknown products **1**−**4** represented an interesting challenge.

Direct chlorination of the CH_2 bridges in **0** and other bicyclo-[1.1.1]pentanes is known but stops after the introduction of two geminal Cl atoms, and forcing conditions cause a destruction of the bicyclic cage.[5] Dilute elemental fluorine is a very powerful

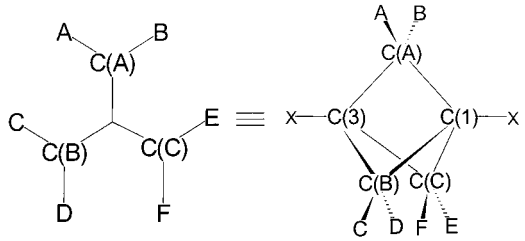

No. X = $COOCH_3$	No. X = H	A	B	C	D	E	F
0	**7**	H	H	H	H	H	H
1	**8**	F	H	H	H	H	H
2a	**9a**	F	H	H	H	F	H
2x	**9x**	F	F	H	H	H	H
2y	**9y**	F	H	H	H	H	F
2z	**9z**	F	H	F	H	H	H
3a	**10a**	F	H	H	F	F	H
3x	**10x**	F	H	H	F	H	F
3y	**10y**	F	F	H	H	F	H
3z	**10z**	F	F	H	H	H	F
4a	**11a**	F	F	H	F	F	H
4x	**11x**	F	F	H	H	F	F
4y	**11y**	F	F	H	F	H	F
4z	**11z**	F	F	F	H	F	H
5	**12**	F	F	F	F	F	H
6	**13**	F	F	F	F	F	F

Figure 1. Structures of compounds **0**−**13**.

[†] University of Colorado.
[‡] Institute of Chemical Technology.

(1) Levin, M. D.; Hamrock, S. J.; Kaszynski, P.; Shtarev, A. B.; Levina, G. A.; Noll, B. C.; Ashley, M. E.; Newmark, R.; Moore, G. G. I.; Michl, J. *J. Am. Chem. Soc.* **1997**, *119*, 12750.
(2) Levin, M. D.; Kaszynski, P.; Michl, J. *Chem. Rev.* **2000**, *100*, 169.
(3) McKinley, A. J.; Ibrahim, P. N.; Balaji, V.; Michl, J. *J. Am. Chem. Soc.* **1992**, *114*, 10631.
(4) Moore, C.; Smith, J. *J. Chem. Soc., Faraday Trans.* **1995**, *91*, 18.

10.1021/ja0000495 CCC: $20.00
Published on Web 03/24/2001

Scheme 1

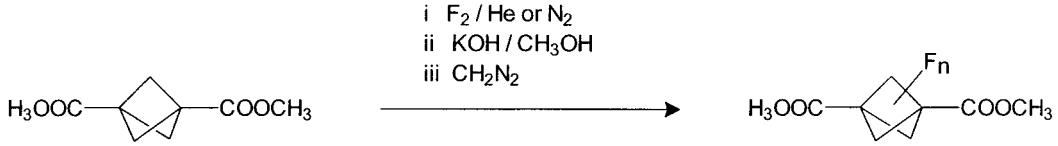

Table 1. Retention Times t_R of **0**−**6** in Capillary GC[a] (see Figure 1)

compd	t_R, min
0	11.16
1	11.55
2a	11.34[b]
2x	10.67
2y	10.97
2z	12.80
3a	10.82
3x	11.57
3y	11.34[b]
3z	9.67
4a	9.97
4x	9.10
4z	11.34[b]
5	8.32
6	7.26

[a] HPB-5 cross-linked capillary column (30 m × 0.33 mm), 80−250 °C (10 °C/min). [b] The retention times of **2a**, **3y**, and **4z** on Fluorcol packed column (21 ft. × 1/4 in.) differ. Typical values at 140 °C (isothermal) are 87.3, 85.7, and 88.4 min, respectively.

fluorinating agent,[6] and even the hexafluorination of **0** proceeds well despite the severe crowding of the six fluorines.[1]

Results and Discussion

The starting material for the preparation of dimethyl bicyclo-[1.1.1]pentane-1,3-dicarboxylate[7,8] is [1.1.1]propellane, and this is made by a reaction first developed in the laboratory of Szeimies.[9] We have now improved the reproducibility of the previously described[7,10] synthetic procedure for this material and raised its yield from ∼75 to ∼100% by optimizing the temperature regime and by using the MeLi complex with LiBr instead of MeLi as the reagent.

Fluorine substitution occurs on the bridge methylene and methyl ester groups with comparable probability, and we found it best to convert all reaction mixtures of esters to diacids and to esterify them with diazomethane before proceeding with analytical and preparative gas chromatography (Scheme 1). The fluorination was monitored by NMR and terminated when the desired degree of substitution was achieved.

Structure Assignment. Elemental analyses and mass spectra leave no doubt about the number of fluorine atoms in the molecule, but the distinction among the isomers of **2**, **3**, and **4** (Figure 1) represents an amusing challenge. Initially, they were characterized only by their distinctive retention times, listed in Table 1, and by their mass spectra. Assuming the absence of rearrangements, the successive bridge fluorination graph of Figure 2 applies. Detection of the products of small-scale fluorination of each of the isolated isomers of **2** and **3** permitted an immediate structural identification of three of the isomers:

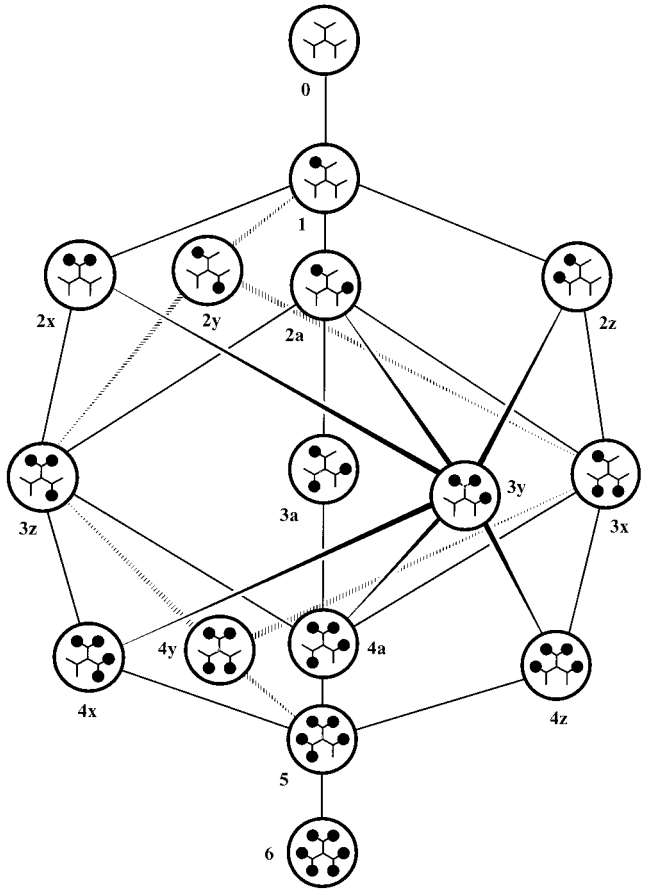

Figure 2. Successive bridge substitution graph for the bicyclo[1.1.1]-pentane cage.

(i) among the difluoro compounds **2**, only **2a** is the precursor to all four trifluorinated compounds **3**, (ii) among the trifluoro compounds **3**, only **3a** yields a sole tetrafluorinated product **4**, and (iii) among the tetrafluoro isomers, only **4a** is formed from all four trifluoro derivatives **3**.

The remaining nine possible isomers of **2**, **3**, and **4** fall into three classes, labeled **x**, **y**, and **z** using a rule reminiscent of the formation of vector product in mathematics. The difluorinated isomers **2x**, **2y**, and **2z** listed in Table 1 were initially named simply in order of increasing retention time. Each of them gives rise to two trifluorinated isomers. The one formed from **2x** and **2y** is called **3z**, the one formed from **2y** and **2z** is called **3x**, and the one formed from **2z** and **2x** is called **3y**. The same procedure is used to label the tetrafluorinated isomers: **4x** is formed from **3y** and **3z**, **4y** is formed from **3x** and **3z**, and **4z** is formed from **3x** and **3y**.

At this point, all isomers listed in Table 1 had labels (**4y** was not detected among the reaction products), and the only degree of freedom left in the structural assignment was the permutation of the labels **x**, **y**, **z** among the families (**2x3x4x**), (**2y3y4y**), and (**2z3z4z**). The **x** family was easy to discriminate from the **y** and **z** families, since **2x** and **4x** only contain CH_2 and CF_2 bridges, while **3x** only contains CHF bridges, and this is not so

(5) Robinson, R. E.; Michl, J. *J. Org. Chem.* **1989**, *54*, 2051.
(6) Adcock, J. L. In Hudlicky, M.; Pavlath, A. E. *Chemistry of Organic Fluorine Compounds II*; ACS Monograph 187; American Chemical Society: Washington, DC, 1995; p 97.
(7) Kaszynski, P.; Michl, J. *J. Org. Chem.* **1988**, *53*, 4593.
(8) Levin, M. D.; Kaszynski, P.; Michl, J. *Org. Synth.* **2000**, *77*, 249.
(9) Semmler, K.; Szeimies, G.; Belzner, J. *J. Am. Chem. Soc.* **1985**, *107*, 6410.
(10) Lynch, K. M.; Dailey, W. P. *Org. Synth.* **1998**, *75*, 98.

Table 2. Observed $^1H-^1H$, $^1H-^{19}F$, and $^{19}F-^{19}F$ Coupling Constants[a] in **1**−**6** (see Figure 1)

					^4J											
		^2J			W path			sickle path						proximate nuclei		
compd	F positions	A−B	C−D	E−F	A−F	B−D	C−E	A−E	A−D	B−F	B−C	D−E	C−F	A−C	B−E	D−F
1	A	*70.5*	2.7	3.3	*27.6*	6.6	9.6	*2.1*	*3.1*	0	0	0	0	*0.9*	0	0
2a	A,E	*68.6*	4.0	*66.3*	*19.4*	6.7	*28.0*	**8.3**	*3.4*	0	0	*2.0*	0	0	*0.5*	0
2x	A,B	**144.2**	2.5	2.5	*19.6*	19.6	10.1	3.2	*0.2*	*0.2*	*3.2*	0	0	*1.5*	*1.5*	0
2y	A,F	*68.9*	3.3	*68.9*	**29.8**	6.6	6.6	*2.1*	*4.7*	*2.1*	0.4	0.4	*4.7*	*0.9*	0	*0.9*
2z	A,C	*65.5*	*65.5*	4.6	*26.0*	7.6	*26.0*	*2.2*	*1.5*	0.4	*1.5*	0.4	*2.2*	**48.9**	0	0
3a	A,D,E	*64.6*	*64.6*	*64.6*	*18.6*	*18.6*	*18.6*	**8.1**	**8.1**	0	0	**8.1**	0	0	0	0
3x	A,D,F	*64.4*	*63.6*	*63.6*	**31.0**	18.2	7.4	*1.6*	**6.9**	*2.0*	0	*0.9*	*1.0*	*0*	0	**63.2**
3y	A,B,E	**141.5**	4.4	*65.2*	*22.7*	*17.3*	*28.4*	**0**	*1.3*	0	*3.3*	*1.0*	0	*1.2*	**52.2**	0
3z	A,B,F	**148.3**	4.0	*69.8*	**14.7**	*18.7*	7.0	*1.2*	*1.0*	**1.0**	*3.4*	0	*6.0*	*1.7*	*0*	*0*
4a	A,B,D,E	**159.0**	*64.8*	*63.2*	*22.7*	**16.6**	*19.2*	**0**	**2.3**	*0*	*0*	**8.5**	0	*1.1*	**63.2**	*0*
4x	A,B,E,F	**144.7**	4.3	**144.7**	**9.7**	*18.1*	*18.1*	**6.0**	2.7	**6.0**	3.3	3.3	2.7	*1.6*	**56.2**	*1.6*
4z	A,B,C,E	**143.0**	*62.8*	*62.8*	*21.1*	*21.1*	**33.5**	**1.3**	*0*	*0*	**1.3**	*2.1*	*2.1*	**66.4**	**66.4**	0
5[b]	A,B,C,D,E	**156.2**	**162.0**	*62.7*	*22.6*	**11.4**	**14.7**	**0**	**4.8**	*0*	**7.8**	**0**	*1.4*	**70.6**	**85.4**	*1.3*
6[b]	A,B,C,D,E,F	**160.4**	**160.4**	**160.4**	**10.3**	**10.3**	**10.3**	**8.6**	**8.6**	**8.6**	**8.6**	**8.6**	**8.6**	**97.9**	**97.9**	**97.9**

[a] J_{HH} are in plain font; J_{HF} are in italics; J_{FF} are in bold; values too small to be measured are marked by zeros. All values were obtained from spectral simulation. [b] Reference 1.

Table 3. Results of $\{^{19}F\}^1H$ and $\{^1H\}^1H$ NOE Measurements (see Figure 1)

	$\{^{19}F\}^1H$ NOE			$\{^1H\}^1H$ NOE	
compd	irradiated nucleus	NOE signals	compd	irradiated nucleus	NOE signals
2x	−119.87	2.56	**1**	1.75	2.22, 5.00
3x	−186.64	5.76		2.22	1.75, 2.31
	−202.12	4.82		2.31	2.22, 3.01
	−216.11	4.69, 5.76		3.01	2.31
3y	−103.00	none		5.00	1.75
	−113.55	2.52	**2a**	1.74	3.02, 4.87
	−170.36	4.77		3.02	1.74
3z	−113.89	5.48	**3y**	1.58	2.52, 4.77
	−135.53	2.73		4.77	1.58
	−212.20	3.14, 5.48	**3z**	2.73	3.14
4a	−109.47	5.35		3.14	2.73
	−116.69	none		5.48	none
	−188.37	5.56			
	−214.66	5.35, 5.56			
4x	−103.34	none			
	−135.53	2.65			

in the **y** and **z** families. The distinction is obvious in the ^1H, ^{19}F, and ^{13}C NMR spectra.

An initial attribution of the remaining two families, **y** and **z**, is possible from the comparison of the NMR spectra of **3y** and **3z** with the previously analyzed[1] spectra of **5** and **6**, which showed large $^4J_{FF}$ coupling constants between proximate F atoms and a large $^4J_{HF}$ coupling constant between W-related H and F atoms. The ^1H and ^{19}F spectra of **3y** and **3z** contain three first-order multiplets due to the CF_2, CHF, and CH_2 groups, and several observations (Table 2) agree that the correct structural assignment is the one shown in Figure 1. The most telling are (i) the huge long-range $^4J_{FF}$ coupling constant of the easily distinguished CHF fluorine in **3y** (52.2 Hz) but not in **3z** (14.7 Hz), which corresponds to a coupling between proximate fluorines, (ii) the large $^4J_{HF}$ coupling constant of the easily distinguished CHF proton in **3y** (22.7 Hz) but not in **3z** (6 Hz), which corresponds to a W coupling path, and (iii) the large $^4J_{HH}$ coupling constant of the CHF proton in **3z** (7.0 Hz) but not in **3y** (too small to be measured), which also corresponds to a W path.

A definitive confirmation of the structural assignment of **3y** and **3z** was obtained from 1-D NOE experiments (Table 3). Thus, irradiation of the CHF proton in **3y** enhances an NOE signal of a proximate CH_2 proton, whereas irradiation of the CHF proton of **3z** does not give any proton NOE signals. This completed the structural assignment of all of the isomers of **1**−**4**, summarized in Figures 1 and 2.

Computed Geometry of Bridge-Fluorinated Bicyclo[1.1.1]-pentanes. Geometry optimizations for all possible bridge-fluorinated bicyclo[1.1.1]pentane isomers showed that the trends in geometry changes found[1] for the transition from hexafluorinated cage to the pentafluorinated one persist with a further decrease in the degree of fluorination (Tables 4−6 and Figure 3, Supporting Information).

For each additional fluorine atom in the cage, the interbridgehead distance, averaged over the isomers **a**, **x**, **y**, and **z**, increases by 0.014 Å. The C(1)−H bonds shorten, the C(2)−C(1)−C(4) angles at the bridgeheads become smaller, and the C(1)−C(2)−C(3) angles at the bridges open up with increasing degree of fluorination (distances between atoms in similar environment and valence angles at similarly substituted atoms were compared). The C−C, C−F, and C(bridge)−H bond lengths and the F−C−F, H−C−F, H−C−H, F−C−C, and H−C−C valence angles depend more on the substitution pattern than on the overall degree of fluorination. The geometry changes correlate with the differences in hybridization calculated from density matrices using Weinhold's natural hybrid orbital procedure (Table 7 and Figure 4, Supporting Information),[11,12] as expected from Bent's rules.[13] For a given degree of fluorination, the C−C bond lengths increase in the order $C-CF_2$, C−CFH, $C-CH_2$.

Computed Strain in Bridge-Fluorinated Bicyclo[1.1.1]-pentanes. Distances between nonbonded proximate H and F atoms calculated in **1**−**5** and measured[1] in **6** (F−F, 2.155−2.580 Å; F−H, 2.008−2.389 Å; H−H, 1.806−2.322 Å) are substantially smaller than the sums of van der Waals radii[14] (F−F, 2.94 Å; F−H, 2.67 Å; H−H, 2.40 Å), but the crowding is not sufficient to displace the H and F atoms out of a single plane. A simple model[1] has been used to evaluate strain energies (SE). The parent bicyclo[1.1.1]pentane **7** was chosen as a reference, and *n*-alkanes and fluorinated *n*-alkanes were taken as standards, strain-free by definition. The SE is equal to the enthalpy change in isodesmic reactions of **7** with 2,2-difluoropropane **14** and 2-fluoropropane **15** to give the bridge-fluorinated

(11) Reed, A. E.; Curtiss, L. A.; Weinhold, F. *Chem. Rev.* **1988**, *88*, 899.
(12) NBO 4.0 Glendening, E. D.; Badenhoop, J. K.; Reed, A. E.; Carpenter, J. E.; Weinhold, F. Theoretical Chemistry Institute, University of Wisconsin, Madison, 1994.
(13) Bent, H. A. *Chem. Rev.* **1961**, *61*, 275.
(14) Bondi, A. *J. Phys. Chem.* **1964**, *68*, 441.

Scheme 2

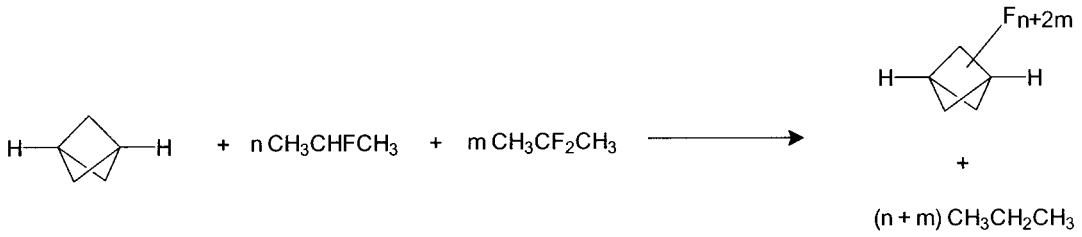

Table 8. Calculated Strain Energy (SE) of **8**−**13** Relative to **7** (see Figure 1)[a]

compd	MP2/6-31G*// MP2/6-31G*	RHF/6-31G*// RHF/6-31G*
7	0	0
8	−0.1	0.2
9a	1.0	0.6
9x	4.2	3.4
9y	3.7	3.0
9z	3.4	3.2
10a	3.4	2.6
10x	7.8	6.7
10y	7.7	7.0
10z	8.6	7.7
11a	12.8	11.7
11x	14.9	13.5
11y	15.7	14.8
11z	15.8	14.3
12	23.3	21.8
13	34.7	32.9

[a] In kcal/mol.

bicyclo[1.1.1]pentanes **8**−**13** and propane **16** (Scheme 2, Table 8). The RHF/6-31G* SE values were usually a little smaller than the MP2/6-31G* values, but the general trends were identical. Zero-point energy corrections were calculated at the MP2/6-31G* level for **9**, and the differences between those corrections for the four isomers were negligible (on the order of 0.2 kcal/mol).

The calculated strain in the cage does not increase evenly with gradual substitution of hydrogen atoms for fluorines. Three "strain-rich" arrangements stand out (Figure 5): geminal, proximate, and W-related. For example, the least strained among the trifluoro derivatives is the symmetrical molecule **10a**, free of strain-rich arrangements (**3a** was actually formed in disproportionally large amounts in the fluorination experiments; the relative fluorination rates of **0**−**5** are presently under examination). The other isomers each contain two strain-rich arrangements and are 4−5 kcal/mol higher in energy. A similar trend is observed in the tetrafluoro derivatives **11**. The isomer **11a**, which contains three "strain-rich" arrangements, is 2−3 kcal/mol less strained than the three other isomers, which contain four such arrangements. The fifth fluorine brings a larger increase of strain into the cage than any previous fluorine but not as much as the sixth one, which introduces three additional strain-rich arrangements and pushes all the structural parameters of the cage to their extremes.

Of the three strain-rich arrangements, two are understood relatively easily in intuitive terms. The CF_2 groups introduce strain via angular distortions, as they attempt to increase the C−C−C valence angles at the bridge, and the proximate arrangement of fluorines causes an increased nonbonded van der Waals repulsion. In contrast, it is not clear what type of interaction is responsible for the very significant SE increase upon introduction of W-related fluorines. Conceivably, it could be the electrostatic interaction of two opposed C−F dipoles.

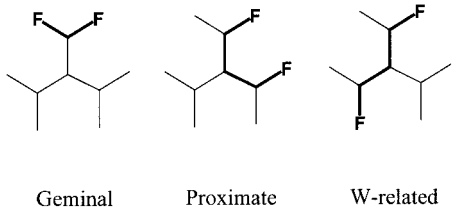

Figure 5. Strain-rich arrangements of fluorine substituents in the bicyclo[1.1.1]pentane cage.

NMR Spectral Assignments. Results obtained from ^{1}H, $\{^1H\}^{13}$C, and ^{19}F NMR spectra of **1**−**4** are collected in Tables 9−11. The assignments relied heavily on $\{^1H\}^1$H and $\{^{19}F\}^1$H NOE measurements (Table 3). To assign the ^{1}H NMR spectrum of **1**, we first performed a ^{1}H−^{13}C HETCOR measurement, which confirmed the already obvious assignment of the multiplet at δ 5.00 ppm to the CHF hydrogen and permitted the four protons responsible for the other multiplets to be grouped into two pairs of protons bound to the same carbon. Subsequent irradiation of the multiplets at 1.75, 2.22, 2.31, 3.01, and 5.00 ppm, and observation of the corresponding NOE signals, provided an unambiguous assignment of these signals to protons H(E), H(F), H(D), H(C), and H(A), respectively (Figure 1).

These experiments also helped to assign signals in the $\{^1H\}^{13}$C spectrum. All carbons in **1** but one appear as doublets, due to spin−spin coupling with fluorine. The assignments of the carbonyl carbon (167.08 ppm) and the methoxy carbon (52.11 ppm, singlet in proton decoupled ^{13}C spectrum) are clear. A^{1}H−^{13}C HETCOR experiment singled out the bridgehead carbons C(1) (43.98 ppm) and the CHF carbon C(A) (96.98 ppm). Results of HETCOR coupled with the results of NOE experiments described above showed that hydrogens H(E) and H(F) are bound to the carbon with a chemical shift of 41.23 ppm, and hydrogens H(D) and H(C) are bound to the carbon with a chemical shift of 45.04 ppm. This allowed us to unambiguously assign signals at 45.04 and 41.23 ppm to C(B) and C(C), respectively (Figure 1). The assignment of spin−spin coupling constants in **1** followed. The comparison of the perturbations in the splitting patterns of different nuclei in the ^{1}H NMR spectrum caused by spin tickling allowed us to determine the relative signs of the following pairs of coupling constants: (i) $^4J_{H(E)F}$ and $^4J_{H(F)F}$ have opposite signs, (ii) $^2J_{H(B)F}$ and $^4J_{H(D)F}$ have the same sign, and (iii) $^4J_{H(C)H(E)}$ and $^4J_{H(C)H(D)}$ have the same sign.

Among the ^{1}H and ^{19}F NMR spectra of the difluoro derivatives **2a**, **x**−**z**, only those of the nonsymmetric structure **2a** are first order. The assignments for **2a** followed from $\{^1H\}^1$H and $\{^{19}F\}^1$H NOE results (Table 3). The two different types of hydrogens in **2x** were distinguished by a $\{^{19}F\}^1$H NOE experiment. Only one of the trifluoro derivatives, **3a**, has second-order ^{1}H and ^{19}F spectra. The compound **3x** has three first-order multiplets at −216.11, −202.12, and −186.64 ppm in the ^{19}F spectrum and 4.69, 4.82, and 5.76 ppm in the ^{1}H spectrum, which correspond to different types of CHF groups. The

Table 9. ^{1}H and ^{19}F NMR Chemical Shifts: Observed in **1** − **5**, and GIAO−RHF/6-31G*//RHF/6-31G* or GIAO−RHF/6-31G*//MP2/6-31G* Calculated in **8** − **12** (see Figure 1)[a]

			δ (ppm), obsd and calcd[b]						
compd	spin system		A	B	C	D	E	F	CH_3
1	first order	obsd	**−181.22**	5.00	3.01	2.31	1.75	2.22	3.70
8		RHF[c]	**−176.89**	5.02	3.19	2.32	1.52	2.01	
8		MP2[d]	**−181.28**	5.08	3.27	2.35	1.56	2.06	
2a	first order	obsd	**−198.07**	5.61	3.02	1.74	**−184.16**	4.87	3.75
9a		RHF[c]	**−187.34**	5.75	2.93	1.46	**−180.81**	4.74	
9a		MP2[d]	**−191.53**	5.85	3.04	1.53	**−184.79**	4.82	
2x	AA′MM′XX′	obsd	**−119.87**	**−119.87**	2.56	2.15	2.56	2.15	3.75
9x		RHF[c]	**−118.51**	**−118.51**	2.50	1.94	2.50	1.94	
9x		MP2[d]	**−121.43**	**−121.43**	2.59	2.00	2.59	2.00	
2y	AA′MM′XX′	obsd	**−215.60**	4.88	3.23	3.23	4.88	**−215.60**	3.74
9y		RHF[c]	**−206.55**	4.70	3.38	3.38	4.70	**−206.55**	
9y		MP2[d]	**−210.94**	4.79	3.49	3.49	4.79	**−210.94**	
2z	AA′MM′XX′	obsd	**−171.57**	5.03	**−171.57**	5.03	1.66	1.66	3.77
9z		RHF[c]	**−165.76**	4.97	**−165.76**	4.97	1.17	1.17	
9z		MP2[d]	**−168.31**	4.80	**−168.31**	4.80	1.24	1.24	
3a	AA′A″XX′X″	obsd	**−201.23**	5.48	5.48	**−201.23**	**−201.23**	5.48	3.82
10a		RHF[c]	**−191.79**	5.47	5.47	**−191.79**	**−191.79**	5.47	
10a		MP2[d]	**−195.82**	5.60	5.60	**−195.82**	**−195.82**	5.60	
3x	first order	obsd	**−216.11**	4.69	5.76	**−186.64**	4.82	**−202.12**	3.82
10x		RHF[c]	**−209.81**	4.39	5.87	**−176.11**	4.60	**−194.82**	
10x		MP2[d]	**−213.97**	4.50	5.98	**−178.15**	4.70	**−197.26**	
3y	first order	obsd	**−113.55**	**−103.00**	2.52	1.58	**−170.36**	4.77	3.80
10y		RHF[c]	**−113.07**	**−102.41**	2.26	1.16	**−166.36**	4.60	
10y		MP2[d]	**−115.83**	**−102.98**	2.40	1.23	**−168.28**	4.70	
3z	first order	obsd	**−135.53**	**−113.89**	2.73	3.14	5.48	**−212.20**	3.78
10z		RHF[c]	**−134.39**	**−115.05**	2.66	3.08	5.48	**−203.63**	
10z		MP2[d]	**−137.25**	**−117.27**	3.22	2.78	5.59	**−207.80**	
4a	first order	obsd	**−109.47**	**−116.69**	5.35	**−214.66**	**−188.37**	5.56	3.85
11a		RHF[c]	**−111.01**	**−116.79**	5.26	**−208.29**	**−178.80**	5.57	
11a		MP2[d]	**−98.77**	**−113.39**	5.39	**−212.32**	**−180.23**	5.71	
4x	AA′MM′XX′	obsd	**−135.53**	**−103.34**	2.65	2.65	**−103.34**	**−135.53**	3.82
11x		RHF[c]	**−133.08**	**−102.90**	2.42	2.42	**−102.90**	**−133.08**	
11x		MP2[d]	**−135.97**	**−103.15**	2.59	2.59	**−103.15**	**−135.97**	
11y	AA′MM′XX′	MP2	**−122.39**	**−122.39**	5.73	**−182.48**	5.73	**−182.48**	
4z	AA′MM′XX′	obsd	**−97.31**	**−97.31**	**−205.62**	4.59	**−205.62**	4.59	3.85
11z		RHF[c]	**−97.09**	**−97.09**	**−198.14**	4.25	**−198.14**	4.25	
11z		MP2[d]	**−97.37**	**−97.37**	**−200.09**	4.36	**−200.09**	4.36	
5	first order	obsd[e]	**−95.96**	**−115.90**	**−118.70**	**−128.68**	**−201.82**	5.88	3.87
12		MP2[d]	**−96.67**	**−116.20**	**−119.93**	**−131.86**	**−197.32**		

[a] ^{1}H NMR chemical shifts are in plain font; ^{19}F NMR chemical shifts are in bold. [b] The formula used for calculation is as follows: ^{1}H NMR $\delta_{calcd} = s(CH_2$ in **7**$) - s_{calcd} + \delta(CH_2$ in **0**$)$, where $\delta(CH_2$ in **0**$)$ is 2.30 ppm (ref 7) and $s(CH_2$ in **7**$)$ is 31.21 (RHF) or 30.80 (MP2); ^{19}F NMR $\delta_{calcd} = s(CF_2$ in **13**$) - s_{calcd} + \delta(CF_2$ in **6**$)$, where $\delta(CF_2$ in **6**$)$ is −116.16 ppm (ref 1) and $s(CF_2$ in **13**$)$ is 364.17 (RHF) or 352.53 (MP2). [c] RHF/6-31G* optimized geometry. [d] MP2-6/31G* optimized geometry. [e] Reference 1.

assignment of the NMR signals was performed by $\{^1H\}^1H$ and $\{^{19}F\}^1H$ NOE experiments (Table 3). Spectra of tetrafluoro derivatives were analyzed in a similar manner. $\{^{19}F\}^1H$ NOE experiments were especially useful in the assignment of ^{19}F NMR signals in **4a** and **4x**.

Comparison of Observed and Calculated Chemical Shifts. The unusual structures of **0**−**6** provide an interesting opportunity to test the performance of the standard methods of calculation of chemical shifts (GIAO-RHF/6-31G*, using RHF/6-31G* and MP2/6-31G* optimized geometries). This is particularly fitting since calculations played an important role in the earlier elucidation of the NMR assignments in **5**.[1] It appeared impractical and unnecessary to perform the calculations on the diesters **0**−**6** themselves, and we have carried them out on the parent structures **7**−**13** (Figure 1), which lack the bridgehead substituents. As was reported earlier,[15,16] the geometries of bicyclo[1.1.1]pentane cages with this type of bridgehead substituents differ only very little from that[17] of the parent bicyclo[1.1.1]pentane. Comparison with the observed chemical shifts is then only for differences relative to **0** for ^{1}H NMR and ^{13}C NMR, and relative to **6** for ^{19}F NMR (for details, see Experimental Section and Calculations). The results are shown in Tables 9 and 10. The calculated relative chemical shifts are in excellent agreement with the experimental values, particularly when MP2 geometries are used, and confirm the spectral assignments made above. The rms errors in calculated relative chemical shifts are ^{1}H, 0.17 ppm (RHF), 0.16 ppm (MP2); ^{13}C, 2.61 ppm (RHF), 1.38 ppm (MP2); ^{19}F, 4.68 ppm (RHF), 3.43 ppm (MP2). The shifts show no simple relation to the calculated natural atomic charges (Table 12 and Figure 4, Supporting Information).

Spin−Spin Coupling Constants. The rich variety of observed long-range coupling constants in **0**−**6** begs for interpretation in structural terms. The ^{1}H−^{1}H, ^{1}H−^{19}F, and ^{19}F−^{19}F coupling constants are summarized in Table 2. The ^{19}F−^{13}C and a few ^{1}H−^{13}C coupling constants are collected in Table 11.

One-bond coupling constants $^1J_{CH}$ and $^1J_{CF}$ in **1**−**4** offer no surprises. The $^1J_{CH}$ values are related to the percent s character (%s) in the carbon hybrid orbital used in the bond (Table 7,

(15) Clauss, A. W.; Wilson, S. R.; Buchanan, R. M.; Pierpont, C. G.; Hendrichson, D. N. *Inorg. Chem.* **1983**, *22*, 628.

(16) Friedli, A. C.; Lynch, V. M.; Kaszynski, P.; Michl, J. *Acta Crystallogr.* **1990**, *B46*, 3771.

(17) Almenningen, A.; Andersen, B.; Nyhus, B. A. *Acta Chem. Scand.* **1975**, *25*, 1271.

Table 10. ^{13}C NMR Chemical Shifts: Observed in **1**−**5** and GIAO-RHF/6-31G*//RHF/6-31G* or GIAO-RHF/6-31G*//MP2/6-31G* Calculated in **8**−**12** (see Figure 1)

		chemical shifts, δ (ppm)			
compd		C(A)[a]	C(B)[a]	C(C)[a]	C(1)[b]
1	obsd	96.98	45.04	41.23	43.98
8	RHF[c]	94.40	47.43	40.12	43.25
8	MP2[d]	96.41	47.92	39.77	43.27
2a	obsd	95.04	32.77	88.41	51.21
9a	RHF[c]	92.80	33.77	85.22	49.82
9a	MP2[d]	95.30	34.17	87.07	49.64
2x	obsd	121.59	42.99	42.99	50.46
9x	RHF[c]	117.74	41.73	41.73	48.15
9x	MP2[d]	121.17	42.26	42.26	48.43
2y	obsd	92.44	37.69	92.44	50.50
9y	RHF[c]	88.04	41.57	88.04	49.21
9y	MP2[d]	90.25	42.46	90.25	49.19
2z	obsd	96.01	96.01	28.91	49.57
9z	RHF[c]	93.86	93.86	28.18	48.33
9z	MP2[d]	95.84	95.84	28.22	48.40
3a	obsd	85.86	85.86	85.86	58.69
10a	RHF[c]	82.75	82.75	82.75	56.30
10a	MP2[d]	84.94	84.94	84.94	56.26
3x	obsd	83.71	94.14	91.39	55.73
10x	RHF[c]	79.47	92.08	87.18	54.18
10x	MP2[d]	81.61	94.41	89.30	54.22
3y	obsd	119.18	29.79	87.89	55.86
10y	RHF[c]	116.27	28.73	85.16	53.25
10y	MP2[d]	119.80	29.10	87.02	53.54
3z	obsd	116.58	34.05	91.98	56.69
10z	RHF[c]	112.14	34.70	87.96	54.09
10z	MP2[d]	115.71	35.50	90.51	54.29
4a	obsd	113.91	83.19	85.61	62.40
11a	RHF[c]	110.28	78.90	82.73	59.40
11a	MP2[d]	113.82	81.21	84.88	59.64
4x	obsd	115.77	31.15	115.77	61.11
11x	RHF[c]	111.58	29.32	111.58	57.88
11x	MP2[d]	115.18	30.01	115.18	58.36
11y	RHF[c]	107.31	87.47	87.47	58.67
11y	MP2[d]	111.05	89.82	89.82	58.96
4z	obsd	118.41	82.35	82.35	60.93
11z	RHF[c]	114.81	79.44	79.44	57.69
11z	MP2[d]	118.33	81.45	81.45	58.01
5	obsd[e]	113.36	110.77	83.30	65.58
12	MP2[d]	114.32	111.17	82.10	65.15

[a] $\delta_{calcd} = s(CH_2 \text{ in } \mathbf{7}) - s_{calcd} + \delta(CH_2 \text{ in } \mathbf{0})$, where δ (CH_2 in **0**) = 52.76 ppm (ref 7) and $s(CH_2 \text{ in } \mathbf{7}) = 158.30$ (RHF) or 156.46 (MP2). [b] $\delta_{calcd} = s(C(1) \text{ in } \mathbf{7}) - s_{calcd} + \delta(C(1) \text{ in } \mathbf{0})$, where δ (C(1) in **0**) = 37.52 ppm (ref 7) and $s(C(1) \text{ in } \mathbf{7}) = 173.81$ (RHF) or 172.23 (MP2). [c] RHF/6-31G* optimized geometry. [d] MP2/6-31G* optimized geometry. [e] Reference 1.

Figure 4, Supporting Information): $|^1J_{CH}| = 17.44 \times (\%s) - 321.33$ (Hz), with a correlation coefficient of 0.963. The $^1J_{CF}$ values are similar to those reported earlier for **5** and **6** and to those familiar from fluorocycloalkanes.[18] They show only a very rough increasing trend with the percent of s character in the C orbital used in the bond and show no correlation with the percent of s character in the fluorine orbital used in the bond. The geminal constants $^2J_{FF}$ are of the usual size, ranging from ∼140 to ∼160 Hz. They show no correlation with the F−F distance. The long-range $^4J_{FF}$ coupling constants are of more interest. Particularly large values occur between proximate fluorines and are among the largest known between aliphatic fluorines.[19−21] This is undoubtedly related to the very short distances between the nonbonded fluorines in these compounds, and we observe

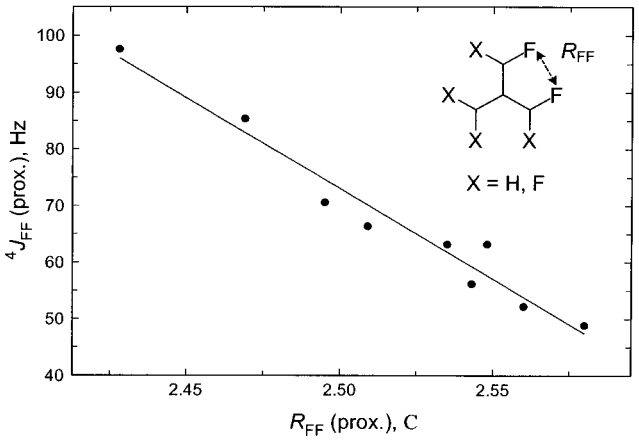

Figure 6. Spin−spin coupling constants of proximate fluorines in **2**−**6** and MP2/6-31G* calculated inter-fluorine distances in **8**−**13**.

an approximate linear relationship between the coupling constants $^4J_{FF}$(prox) in **2z**-**6** and the distance R_{FF}(prox) between proximate fluorines calculated in **9z**-**13**: $|^4J_{FF}(\text{prox})| = -3.20 \times R_{FF}(\text{prox}) + 872.5$, with R in pm and J in Hz, with a correlation coefficient of 0.978 (Figure 6). The $^4J_{FF}$ constants between W-related fluorines are unusually large and vary by more than a factor of 3 without an immediately apparent reason. The $^4J_{FF}$ constants between sickle-related fluorines are smaller and even more widely variable in a seemingly random way.

The $^4J_{HF}$ constants between proximate hydrogen and fluorine observed in **1**−**5** are all small (0−1.6 Hz) and unrelated to the distance between hydrogen and fluorine calculated in **8**−**12** (2.234−2.390 Å). It was suggested earlier[1] that although short in absolute terms, the HF distances are still too large for the mechanism of through-space spin−spin coupling to operate, or else through-space and through-bond contributions cancel. The $^4J_{HF}$ constants between W-related atoms are very large and more uniform (17−28 Hz) than the corresponding $^4J_{FF}$ constants. The $^4J_{HF}$ constants between sickle-related atoms are smaller and widely variable.

Comparison of Observed and Calculated Spin−Spin Coupling Constants. Bicyclo[1.1.1]pentane **7** has been previously recognized as an especially intriguing challenge to the theory of spin−spin coupling in molecules,[22,23] and it has been noted that the calculated magnitudes of coupling constants depend strongly on the size of the basis set used.[22] As usual, the Fermi contact (FC) term was found to be dominant for ^{1}H−^{1}H coupling.[22]

With a hopefully simple understanding of the intuitively nonobvious pattern of coupling constants in **1**−**6** as the ultimate goal, we have used the equation-of-motion coupled cluster method with single and double excitations (EOM-CCSD) developed in Bartlett's group[24,25] to calculate the spin−spin coupling constants in **8** and **9y** (Tables 13 and 14), using MP2/6-311G* optimized geometries. These were nearly identical to the MP2/6-31G* optimized geometries except that the C−F bonds were ∼0.01 D shorter. The purpose was to reproduce the observed values as closely as possible and to find out whether one of the four recognized mechanisms of isotropic

(18) For a compilation of coupling constants, see: Emsley, J. W.; Phillips, L.; Wray, V. *Prog. Nucl. Magn. Reson. Spectrosc.* **1975**, *10*, 83.
(19) Weigert, F. J.; Roberts, J. D. *J. Am. Chem. Soc.* **1968**, *90*, 3577.
(20) Banks, R. F.; Bridge, M.; Fields, R.; Haszeldine, R. N. *J. Chem. Soc. C* **1971**, 1282.
(21) Servis, K. L.; Fang, K.-N. *J. Am. Chem. Soc.* **1968**, *90*, 6712.
(22) Lazzaretti, P.; Malagoli, M.; Zanasi, R.; Della, E. W.; Lochert, I. J.; Giribet, C. G.; Ruiz de Azua, M. C.; Contreras, R. H. *J. Chem. Soc., Faraday Trans.* **1995**, *91*, 4031.
(23) Della, E. W.; Lochert, I. J.; Peruchena, N. M.; Aucar, G. A.; Contreras, R. H. *J. Phys. Org. Chem.* **1996**, *9*, 168.
(24) Perera, S. A.; Nooijen, M.; Bartlett, R. J. *J. Chem. Phys.* **1996**, *104*, 3290.
(25) Perera, S. A.; Sekino, H.; Bartlett, R. J. *J. Chem. Phys.* **1994**, *101*, 2186.

Table 11. Observed $\{^1H\}^{13}C$ NMR Chemical Shifts and J_{CF} Coupling Constants in **1**−**6** (see Figures 1 and 2)

	chemical shift,[a] multiplicity, J_{CF}[b]					
compd	C(A)	C(B)	C(C)	C(1)[c]	C═O	CH_3
1	96.98, d (244.0)	45.04, d (10.2)	41.23, d (18.2)	43.98, d (21.0)	167.08, d (1.5)	52.11, s
2a[d]	95.04, dd (238.3, 12.4)	32.77, dd (16.7, 13.1)	88.41, dd (248.5, 16)	51.21, t (20.3)	164.79, t (1.5)	52.41, s
2x	121.59, t (296.5)	42.98, t (6.2)	42.98, t (6.2)	50.46, t (19.6)	164.79, t (1.5)	52.39, s
2y	92.44, dd (242.0, 37.8)	37.69, t (16.0)	92.44, dd (242.0, 37.8)	50.50, t (20.3)	164.77, t (1.5)	52.46, s
2z	96.01, dd (264.0, 13.0)	96.01, dd (264.0, 13.0)	28.91, t (20.3)	49.57, t (20.7)	164.69, t (1.5)	52.52, s
3a	85.86, dt (244.0, 16.7)	85.86, dt (244.0, 16.7)	85.86, dt (244.0, 16.7)	58.69, q (20.3)	162.82, q (1.5)	52.74, s
3x	83.71, ddd (245.2, 38.8, 19.6)	94.14, ddd (249.2, 20.3, 6.5)	91.39, ddd (250.6, 34.8, 4.4)	55.73, ddd (21.2, 19.7, 18.2)	162.68, q (1.4)	52.87, s
3y[e]	119.18, dd (305.2, 292.1)	29.68, ddd (16.7, 9.9, 5.8)	87.79, dd (260.2, 8.0)	55.67, q (19.6)	162.46, q (1.5)	52.61, s
3z	116.58, ddd (295, 290, 31.6)	34.05, ddd (16.7, 8.7, 6.5)	91.98, ddd (237.6, 19, 6.0)	56.69, dt (21, 19.6)	162.43, q (1.4)	52.67, s
4a	113.91, dddd (303, 293, 30,2)	83.19, dddd (245, 21, 15, 8.7)	85.61, dddd (254, 24, 7.3, 2)	62.4, tt (20, 19)	160.56, p (1.5)	53.06, s
4x	115.77, m AMM′XX′	31.15, tt (10.3, 6.5)	115.77, m AMM′XX′	61.11, tt (20.7, 19.3)	160.34, p (1.5)	52.99, s
5[f]	113.36, m (303, 301, 2, 22, 2, 20)	110.77, m (291, 305, 5, 30, 33)	83.30, m (258, 17, 7)	65.58, h (19)	158.42[g]	53.34[g]
6[f]	110.26, m AXX′YY′Y″Y‴ (299.3, 25.1, 4.0)	110.26, m AXX′YY′Y″Y‴ (299.3, 25.1, 4.0)	110.26, m AXX′YY′Y″Y‴ (299.3, 25.1, 4.0)	68.79[g]	156.45[g]	53.54[g]

[a] δ, ppm. [b] In hertz. [c] Bridgehead. [d] J_{CH} (Hz): C(A) 190.4, 14.6, 12.1, 8.7, C(B) 162.2, 152.3, 7.3, 5.8, C(C) 194.4, 25.6, 12.4, 3.3. [e] J_{CH} (Hz): C(A) 21.4, 18.3, 8.9, C(B) 163.5, 153, 7.6, C(C) 193.4, 25.5,13.4. [f] Reference 1. [g] The splitting pattern and coupling constants have not been reported.

Table 13. EOM-CCSD/6-311G*//MP2/6-311G* Calculated Spin−Spin Coupling Constants in **8** (Hz)

	individual contributions					
	PSO	DSO	FC	SD	total	exp (**1**)[a]
$^2J_{H(C)H(D)}$	1.6982	−2.2876	−4.4696	0.2759	−4.7831	2.7[b]
$^2J_{H(E)H(F)}$	1.7667	−2.3807	−5.2448	0.2661	−5.5927	3.3
$^4J_{H(B)H(D)}$ W	1.7815	−2.3617	4.7488	0.0062	4.1748	6.6
$^4J_{H(B)H(E)}$	−1.4728	1.8175	−0.3412	0.0582	0.0617	0
$^4J_{H(C)H(E)}$ W	1.7914	−2.3471	6.9098	0.0065	6.3606	9.6[b]
$^4J_{H(D)H(F)}$	−1.4611	1.7409	−0.3912	0.0472	−0.0642	0
$^2J_{H(B)F}$	5.8156	−0.9191	59.6731	−3.2532	61.3164	70.5[c]
$^4J_{H(C)F}$	−0.1210	1.2297	0.6068	−0.1948	1.5207	0.9
$^4J_{H(D)F}$	1.4445	−1.6167	2.0833	−0.2168	1.6943	3.1[c]
$^4J_{H(E)F}$	−0.4530	−1.3806	−1.3920	0.1085	−3.1171	2.1[d]
$^4J_{H(F)F}$ W	0.5896	−1.7895	20.5283	0.0781	19.2503	27.6[d]
$^1J_{FC(2)}$	15.2578	0.9326	−253.8589	14.0459	−223.6226	244.0
$^2J_{FC(1)}$	2.2966	−0.500	13.5194	1.7686	17.0846	21.0
$^3J_{FC(4)}$	−3.1862	−0.4071	19.6889	0.1133	16.2089	18.2
$^3J_{FC(5)}$	−0.9137	0.0560	10.7890	−0.5550	9.3763	10.2

[a] Absolute values of observed coupling constants. [b] These two coupling constants have the same signs. [c] These two coupling constants have the same signs. [d] These two coupling constants have opposite signs.

nuclear spin−spin coupling dominates: FC, spin−dipole (SD), paramagnetic spin−orbit (PSO) or diamagnetic spin−orbit (DSO). If there is a dominant mechanism, it may lead us to a recognizable and understandable correlation with the molecular structure.

In a preliminary calculation performed with the 6-31G* basis set, we found that although the trends in the coupling constants were described correctly, the quantitative agreement of calculated values with the experimental results was poor. We subsequently adopted the 6-311G* basis set and found that the calculated values then became closer to those observed. Still, the mean percent errors were 54.3% for J_{HH}, 41.2% for J_{HF}, and 11.5% for J_{FC} in **8** and 83.7% for J_{HH}, 38.3% for J_{HF}, 19.0% for J_{FF}, and 10.9% for J_{CF} in **9y**, with the $^2J_{HH}$ values too large and the W-path $^4J_{HH}$ and $^4J_{HF}$ values too small. Of the three measured relative signs, the two J_{HF} pairs agreed well, but the calculation failed to reproduce the equal signs of $^2J_{H(C)H(D)}$ and $^2J_{H(C)H(E)}$. It is possible that some of the discrepancies between experimental and calculated data are due to the differences in the geometries of **1** and **2y** on one hand and **8** and **9y** on the other, even though these are presumably only slight.

Of the four terms that contribute to the coupling constants (Tables 13 and 14), the SD term is of very minor importance. The sum of the usually opposed paramagnetic and diamagnetic spin−orbit (PSO and DSO, respectively) contributions to J_{HH} and J_{HF} generally is an order of magnitude smaller than the FC contribution except when the total J value is below 1−2 Hz, and it seems adequate to base the consideration of trends in these coupling constants on the FC term alone as is customary (taken individually, the PSO and DSO contributions are by no

Table 14. EOM-CCSD/6-311G*//MP2/6-311G* Calculated Spin−Spin Coupling Constants in **9y** (Hz)

	individual contributions					
	PSO	DSO	FC	SD	total	exp (**2y**)[a]
$^2J_{H(C)H(D)}$	1.5566	−2.1028	−5.0476	0.2965	−5.2973	3.3
$^4J_{H(B)H(C)}$	1.6096	−2.2257	−0.3766	−0.0236	−1.0163	0.4
$^4J_{H(B)H(E)}$	−1.5378	1.9587	−0.2868	0.0653	0.1994	0
$^4J_{H(C)H(E)}$ W	1.7800	−2.3466	4.7489	0.0089	4.1912	6.6
$^2J_{H(B)F(A)}$	6.6140	−0.8417	57.9156	−3.2613	60.4266	68.9
$^4J_{H(B)F(F)}$	0.2233	−1.3054	−1.7250	0.0829	−2.7242	2.1
$^4J_{H(C)F(A)}$	0.0119	1.3362	0.4672	−0.1955	1.6198	0.9
$^4J_{H(D)F(A)}$	1.6627	−1.5438	3.3571	−0.2432	3.2328	4.7
$^4J_{F(A)F(F)}$ W	−40.6852	−1.3318	1.6478	3.5947	−36.7745	29.8
$^1J_{FC}$	17.2358	0.9586	−250.4899	14.1558	−218.1397	242.0

[a] Absolute values of observed coupling constants.

means negligible relative to FC). In contrast, the long-range $^4J_{FF}$ coupling constant along the W path in **2y** is entirely dominated by the PSO contribution. We believe that calculations for additional members of the family **0**−**6** are needed before we can attain the ultimate goal stated above, but they will require considerable additional computational effort and lie outside the scope of the present paper.

Conclusions. Of the 16 possible dimethyl bicyclo[1.1.1]-pentane-1,3-dicarboxylates with H and/or F atoms on the three bridges, 15 are now known. Calculated cage geometries and strain energies depend on the substitution pattern in a regular way, with three fluorine arrangements especially energy-rich: geminal, proximate, and W-related. The ^{1}H, ^{13}C, and ^{19}F spectra of **1**−**6** have been assigned and exhibit a striking variety of chemical shifts and long-range spin−spin coupling constants. For the purpose of comparison with calculations, the effect of bridgehead carbomethoxy substituents has been neglected. Nevertheless, the chemical shifts are reproduced very well by GIAO-HF/6-31G* results. The agreement of the coupling constants with EOM-CCSD/6-311G*//MP2/6-311G* results for two of the compounds is only semiquantitative. The observed constants do not show a recognizable pattern, except that the $^4J_{FF}$ coupling constants between proximate fluorine atoms are particularly large and show inverse linear correlation with the calculated inter-fluorine distance.

Experimental Section and Calculations

General Procedures. NMR spectra were measured in $CDCl_3$ unless otherwise indicated. ^{19}F and ^{13}C NMR spectra were obtained at 376.5 and 100 MHz, respectively, with a Bruker 400 spectrometer. ^{1}H NMR spectra were obtained at 400.1 and 300 MHz with Bruker 400 and Varian VXR 300 spectrometers, respectively. $CDCl_3$, $CHCl_3$, and $CFCl_3$ were used as internal standards for ^{13}C, ^{1}H, and ^{19}F NMR spectra, respectively. Positive shifts are downfield and are expressed relative to TMS (^{1}H and ^{13}C) and $CFCl_3$ (^{19}F). $\{^{19}F\}^1H$ NOE experiments were performed on a Varian Unity Inova 500 spectrometer using a Nalorac four-nucleus probe which allows simultaneous detection of ^{1}H and ^{19}F. IR spectra were recorded on neat samples of liquids and in KBr pellets for solids with a Perkin-Elmer 1600 Series FTIR instrument. An HP 5988A GCMS instrument was used for EIMS measurements. High-resolution mass spectra were taken on a VG 7070EQ instrument. Elemental analysis was performed by Analytic Laboratories, University of California, Berkeley, CA, or Desert Analytics, Tucson, AZ. Analytical GC was carried out on a HPB-5 cross-linked capillary column (30 m × 0.33 mm). Preparative GC was carried out on a SE-30 (20% on Chromosorb WPH 80/100) 21 ft × 3/16 in. column or a SE-52 (5% on Chromosorb WPH 80/100) 21 ft × 1/4 in. column. The substances are colorless liquids except where the melting point is given.

Calculations. Unconstrained geometry optimization (RHF/6-31G* and MP2/6-31G*) and NMR chemical shift calculations (GIAO-RHF/6-31G*) at both sets of optimized geometries were carried out for **7**−**13** using the GAUSSIAN 94 program[26] with an IBM RISC 6000-590 workstation. For **8** and **9y**, the geometries were also optimized at the MP2/6-311G* level. For comparison with observed chemical shifts, the s_{calcd} results obtained for **7** − **13** were expressed relative to **0** and **6**, using the following formulas. ^{1}H NMR: $\delta_{calcd} = s(CH_2 \text{ in } \mathbf{7}) - s_{calcd} + \delta(CH_2 \text{ in } \mathbf{0})$, where δ (CH_2 in **0**) is 2.30 ppm.[7] ^{19}F NMR: $\delta_{calcd} = s(CF_2 \text{ in } \mathbf{13}) - s_{calcd} + \delta(CF_2 \text{ in } \mathbf{6})$, where δ (CF_2 in **6**) is −116.16 ppm.[1] ^{13}C NMR: $\delta_{calcd} = s(CH_2 \text{ in } \mathbf{7}) - s_{calcd} + \delta(CH_2 \text{ in } \mathbf{0})$, where δ (CH_2 in **0**) = 52.76 ppm,[7] $\delta_{calcd} = s(C(1) \text{ in } \mathbf{7}) - s_{calcd} + \delta(C(1) \text{ in } \mathbf{0})$, where δ (C(1) in **0**) = 37.52 ppm.[7]

Spin−spin coupling constants in **8** and **9y** were calculated by the EOM-CCSD/6-311G* method at MP2/6-311G* optimized geometries with the ACES II program[27] and an HP Exemplar S2200 computer.

NMR simulations and iterations were performed with a PERCH 2/95 program[28] and a 486/40 MHz/8 Mb RAM IBM-compatible PC.

[1.1.1]Propellane Solution in Ether. To a stirred and cooled (−50 °C) mixture of 147 g (0.505 mol) of 1,1-dibromo-2,2-bis(chloromethyl)-cyclopropane,[9] 130 mL of pentane, and 20 mL of diethyl ether in a 2-L four-necked round-bottom flask equipped with a mechanical stirrer, a thermometer, a septum, and an adapter to a dry ice condenser, is added 800 mL of a 1.5 M solution of methyllithium complex with lithium bromide in diethyl ether through a wide cannula (i.d. ≥ 2 mm) directly from the commercial bottle (Aldrich) capped with a Sure-Seal stopper, at such a rate that temperature does not exceed −45 °C. The first 10 mL are added over a period of at least 5 min, and the remainder at a gradually increasing rate compatible with keeping the temperature of the reaction mixture at −50 °C. The addition rate is regulated by lowering the cannula below the liquid level in the bottle or withdrawing it from the liquid, with a constant flow of inert gas through the system. Temperature control is essential (if the reaction runs above −40 °C, the yield will be reduced; below −50 °C the reaction is slow, MeLi may accumulate, and the mixture will eventually overheat). After the addition is finished, the dry ice cooling bath is replaced with an ice bath. The reaction mixture is stirred at 0−3 °C until interruption of stirring causes the solution to clear and insoluble material to precipitate (about 1.5 h). Volatile materials are distilled into a dry ice cooled 2 L

(26) Gaussian 94, Revision C.2. Frisch, M. J.; Trucks, G. W.; Schlegel, H. B.; Gill, P. M. W.; Johnson, B. G.; Robb, M. A.; Cheeseman, J. R.; Keith, T.; Peterson, G. A.; Montgomery, J. A.; Raghavachari, K.; Al-Laham, M. A.; Zakrzewski, V. G.; Ortiz, J. V.; Foresman, J. B.; Cioslowski, J.; Stefanov, B. B.; Nanayakkara, A.; Challacombe, M.; Peng, C. Y.; Ayala, P. Y.; Chen, W.; Wong, M. W.; Andres, J. L.; Replogle, E. S.; Gomperts, R.; Martin, R. L.; Fox, D. J.; Binkley, J. S.; Defrees, D. J.; Baker, J.; Stewart, J. P.; Head-Gordon, M.; Gonzalez, C.; Pople, J. A. Gaussian, Inc., Pittsburgh PA, 1995.

(27) ACES II is a program product of the Quantum Theory Project, University of Florida. Authors: Stanton, J. F.; Gauss, J.; Watts, J. D.; Nooijen, M.; Oliphant, N.; Perera, S. A.; Szalay, P. G.; Lauderdale, W. J.; Kucharski, S. A.; Gwaltney, S. R.; Beck, S.; Balková, A.; Bernholdt, D. E.; Baeck, K. K.; Rozyczko, P.; Sekino, H.; Hober, C.; Bartlett, R. J. Integral packages included are VMOL (Almlöf, J.; Taylor, P. R.), VPROPS (Taylor, P. R.), and ABACUS (Helgaker, T.; Jensen, H. J. Aa.; Jørgensen, P.; Olsen, J.; Taylor, P. R.).

(28) Laatikainen, R.; Niemitz, M.; Sundelin, J.; Hassinen, T. *An Integrated Software for Analysis of NMR Spectra on PC*; Version 2/95, September 1995. PERCH Project, University of Kuopio, Kuopio, Finland, 1993−1995.

round-bottom Pyrex receiver flask containing a magnetic stirring bar. The distillation pressure is gradually reduced from atmospheric to that of a water aspirator at a rate that keeps the temperature of the boiling liquid at 0 °C or below. The distillate contains ~2 equiv of MeBr for each equiv of [1.1.1]propellane (^{1}H NMR signals of comparable intensity at δ 2.6 and δ 2.0, respectively). The yield of [1.1.1]propellane is essentially quantitative as estimated from ^{1}H NMR and titration with I_2/CCl_4. The reaction runs equally well on a smaller scale, as long as a freshly opened bottle of MeLi solution is used. The addition of the methyllithium solution is then best carried out from an addition funnel, which permits easier control over the rate of addition. The diester **0** was prepared from this solution in three steps as described elsewhere.[8]

Direct Fluorination of Dimethyl Bicyclo[1.1.1]pentane-1,3-dicarboxylate[8] (0). Caution: *Fluorine is hazardous. Extreme care should be exercised. All manipulations must be performed in a well-ventilated hood. Excess fluorine should be trapped in activated CaO.*

Method A. Fluorine (5% in helium) was bubbled (40−96 mmol, 30 mL/min) into the solution of dimethyl bicyclo[1.1.1]pentane-1,3-dicarboxylate (**0**) (1.5 g, 8.15 mmol) in 250 mL of 1,1,2-trichlorotrifluoroethane until the desired extent of fluorination was reached (10−24 h), as determined by ^{1}H and ^{19}F NMR. Excess fluorine was trapped in activated CaO. The solvent was evaporated, and the residue was refluxed for 0.5 h in a solution of KOH (2.3 g) in aqueous methanol (50 mL). The solvent was partially evaporated, aqueous H_2SO_4 (6 mL, 20% w/w) was added, and the solution was extracted with a benzene−THF (9:1) mixture (6 × 200 mL). The extract was washed with saturated aqueous NaCl. The solvents were evaporated, and a solution of diazomethane,[29] obtained from *p*-tolylsulfonylmethylnitrosamide (3.2 g) in ether (50 mL) and KOH (0.6 g) in 96% EtOH (15 mL), was added to the crude product (1.3 g). In a typical example, after evaporation of ether, the residue (1.5 g, 6.6 mmol, 80%) contained a mixture of **1** (7%), **2a-z** (42%), **3a-z** (45%), **4a-z** (6%), and **5** (<0.3%) (by ^{19}F NMR). It was separated on a silica gel column with a CH_2Cl_2−EtOAc (35:1) mixture as eluent and further purified by preparative GC. ^{1}H, ^{19}F, and ^{13}C NMR spectral data are collected in Tables 9−11.

Method B. A solution of **0** (0.5 mmol) in 1,1,2-trichlorotrifluoroethane (20 mL) was placed in a pressurized glass flask equipped with a valve and a pressure gauge. The flask was then charged with an F_2/N_2 (10% w/w) mixture to the pressure of 30−60 psi depending on the desired degree of fluorination. The contents of the flask were vigorously stirred with a magnetic stirrer at ambient temperature. The residual fluorine was trapped in activated CaO, and the reaction mixture was worked up as described above. When the reaction was performed on a scale of less than 10 mg, the residue after evaporation of the solvent was treated with excess of methanol (10 mL) and the solvent was evaporated. The products were analyzed by GC.

Dimethyl 2-Fluorobicyclo[1.1.1]pentane-1,3-dicarboxylate (1). Colorless crystals: mp 53 °C; IR 3024, 2953, 1736, 1437, 1384, 1306, 1223, 1096, 1060, 927. EIMS *m*/*z* 203 $[M + H]^+$ (1), 188 (2), 170 (62), 142 (95), 114 (83), 99 (18), 84 (78), 63 (62), 59 (100), 57 (61), 39 (59), 29 (28). HRMS calcd for $[M + H]^+$ 203.0719, obsd 203.0770. Anal. Calcd for $C_9H_{11}FO_4$: C, 53.47; H, 5.48. Found: C, 53.24; H, 5.37.

Dimethyl 2,4-*trans*-Difluorobicyclo[1.1.1]pentane-1,3-dicarboxylate (2a). IR 3003, 2961, 1739, 1440, 1348, 1316, 1227, 1142, 1088, 1041, 932. EIMS *m*/*z* 220 M^+ (0.5), 205 $[M - CH_3]^+$ (1), 189 $[M - OCH_3]^+$ (39), 160 (79), 132 (57), 117 (49), 111 (33), 101 (38), 85 (26), 69 (42), 63 (67), 59 (100), 57 (58), 43 (69), 41 (47), 28 (40). HRMS calcd $[M + H]^+$ 221.0625, obsd 221.0611. Anal. Calcd for $C_9H_{10}F_2O_4$: C, 49.10; H, 4.58. Found: C, 48.86; H, 4.29.

Dimethyl 2,2-Difluorobicyclo[1.1.1]pentane-1,3-dicarboxylate (2x). IR 3039, 3002, 2961, 1739, 1508, 1440, 1388, 1318, 1276, 1223, 1160, 1129, 1082, 995, 961. EIMS *m*/*z* 189 $[M - OCH_3]^+$ (32), 160 (74), 132 (62), 117 (51), 111 (31), 101 (36), 69 (43), 63 (71), 59 (100), 57 (55). Anal. Calcd for $C_9H_{10}F_2O_4$: C, 49.10; H, 4.58. Found: C, 48.78; H, 4.32.

Dimethyl 2-r-4-*cis*-*exo*-Difluorobicyclo[1.1.1]pentane-1,3-dicarboxylate (2y). Colorless crystals: mp 95 °C. IR 3143, 3048, 2962, 1738, 1442, 1408, 1320, 1239, 1216, 1111, 1067. EIMS *m*/*z* 205 $[M - CH_3]^+$ (0.5), 189 $[M - OCH_3]^+$ (42), 160 (78), 132 (63), 117 (56), 101 (39), 85 (28), 59 (100). Anal. Calcd for $C_9H_{10}F_2O_4$: C, 49.10; H, 4.58. Found: C, 48.94; H, 4.41.

Dimethyl 2-r-4-*cis*-*endo*-Difluorobicyclo[1.1.1]pentane-1,3-dicarboxylate (2z). Colorless crystals: mp 94 °C. IR 3012, 2961, 1739, 1436, 1384, 1323, 1239, 1217, 1174, 1113, 1099, 1069, 955. EIMS *m*/*z* 189 (32), 188 (43), 160 (100), 132 (90), 117 (77), 102 (58), 63 (55), 17 59 (80). HRMS calcd for $[M + H]^+$ 221.0625, obsd 221.0632. Anal. Calcd for $C_9H_{10}F_2O_4$: C, 49.10; H, 4.58. Found: C, 48.87; H, 4.36.

Dimethyl 2-r-4-*trans*-5-*trans*-Trifluorobicyclo[1.1.1]pentane-1,3-dicarboxylate (3a). Colorless crystals: mp 66 °C. IR 2851, 1739, 1456, 1377, 1323, 1230, 1123, 1088, 1045, 933. EIMS *m*/*z* 238 M^+ (1), 207 $[M\text{-}OCH_3]^+$ (30), 189 (12), 178 (33), 160 (29), 150 (26), 135 (37), 120 (22), 101 (34), 75 (42), 63 (100), 59 (100), 51 (41), 39 (26), 29 (39). HRMS calcd for $[M + H]^+$ 239.0531, obsd 239.0521. Anal. Calcd for $C_9H_9F_3O_4$: C, 45.39; H, 3.81. Found: C, 45.16; H, 3.66.

Dimethyl *2*-r-*4-cis*-*exo*-5-*trans*-Trifluorobicyclo[l.1.1 pentane-1,3-dicarboxylate (3x). IR 3022, 2963, 1733, 1436, 1382, 1370, 1318, 1233, 1118, 1070, 973, 939. EIMS *m*/*z* 207 (17), 178 (32), 174 (20), 163 (14), 150 (21), 135 (28), 120 (18), 75 (20), 63 (100), 59 (42). HRMS calcd for $[M + 1]^+$ 239.0531, obsd 239.0523. Anal. Calcd for $C_9H_9F_3O_4$: C, 45.39; H, 3.81. Found: C, 45.21; H, 3.69.

Dimethyl 2,2-r-4-*endo*-Trifluorobicyclo[1.1.1]pentane-1,3-dicarboxylate (3y). Synthesized from **2a** by method B. IR 3010, 2959, 1739, 1436, 1384, 1322, 1238, 1217, 1183, 1058, 953. EIMS *m*/*z* 207 (0.5), 178 (43), 163 (40), 135 (25), 120 (31), 63 (100), 59 (67). HRMS calcd for $[M + H]^+$ 239.0531, obsd 239.0547. Anal. Calcd for $C_9H_9F_3O_4$: C, 45.39; H, 3.81. Found: C, 45.52; H, 3.98.

Dimethyl 2,2-r-4-*exo*-Trifluorobicyclo[1.1.1]pentane-1,3-dicarboxylate (3z). Colorless crystals: mp 56 °C. IR 2951, 1742, 1443, 1384, 1328, 1287, 1226, 1187, 1080, 982, 958, 949. EIMS *m*/*z* 239 (3), 207 (33), 178 (100), 163 (40), 135 (95), 63 (52), 59 (59). HRMS calcd for $[M + H]^+$ 239.0531, obsd 239.0550. Anal. Calcd for $C_9H_9F_3O_4$: C, 45.39; H, 3.81. Found: C, 45.22; H, 3.61.

Dimethyl 2,2-r-4-*exo*-5-*endo*-Tetrafluorobicyclo[1.1.1]pentane-1,3-dicarboxylate (4a). IR 3012, 2965, 1747, 1441, 1374, 1330, 1296, 1230, 1192, 1149, 1078, 992, 954. EIMS *m*/*z* 257 (0.5), 226 $[M - OCH_3]^+$ (7), 197 (74), 182 (21), 154 (100), 78 (45). Anal. Calcd for $C_9H_8F_4O_4$: C, 42.20; H, 3.15. Found: C, 41.97; H, 3.03.

Dimethyl 2,2,4,4-Tetrafluorobicyclo[1.1.1]pentane-1,3-dicarboxylate (4x). IR 3018, 2965, 1747, 1495, 1441, 1404, 1335, 1305, 1225, 1155, 1106, 1066, 970. EIMS *m*/*z* 226 $[M - OCH_3]^+$ (4), 197 (34), 182 (51), 154 (41), 78 (100). Anal. Calcd for $C_9H_8F_4O_4$: C, 42.20; H, 3.15. Found: C, 42.46; H, 3.31.

Dimethyl 2,2,4-*endo*-5-*endo*-Tetrafluorobicyclo[1.1.1]pentane-1,3-dicarboxylate (4z). Synthesized from a mixture of **3b** and **3c** by method B. IR 3016, 2965, 1746, 1442, 1368, 1329, 1294, 1172, 1131, 1064, 992, 953. EIMS *m*/*z* 257 (1), 226 (14), 197 (23), 182 (13), 169 (18), 154 (21), 120 (11), 101 (7), 63 (100). Anal. Calcd for $C_9H_8F_4O_4$: C, 42.20; H, 3.15. Found: C, 42.52; H, 3.34.

Acknowledgment. This project was supported by the U.S. National Science Foundation (CHE-9819179) and the U.S.−Czechoslovak Science and Technology Program (Grant 94037). We are grateful to Prof. R. J. Bartlett for making available to us a copy of the ACES II program.

Supporting Information Available: Tables of calculated interatomic distances and valence angles in **7**−**13**, calculated percent of p character in natural atomic hybrids at carbon atoms in **7**−**13**, and calculated natural atomic charges in **7**−**13**. This material is available free of charge via the Internet at http://pubs.acs.org.

JA0000495

(29) Furniss, B. S., Hannaford, A. J., Smith, P. W. G., Tatchell, A. R., Eds. *Vogel's Textbook of Practical Organic Chemistry*, 5th ed.; Longman: Essex, UK, p 432.